Estimation of turbulence parameters from solar observations

Lyes LAKHAL*[a], Abdanour IRBAH*[a], Claude AIME**[b], Julien BORGNINO**[b], François MARTIN**[b]

[a]CRAAG - *Observatoire d'Alger*; [b]UMR 6525 Astrophysique, Université de Nice-Sophia Antipolis

ABSTRACT

The one-dimensional point spread function for long-exposure frames of the whole system atmosphere – instrument is calculated from solar limb observations using data recorded at OCA Observatory (France). It is then compared to the theoretical one deduced from the Von Karman model and various wave-front structure functions. Good agreement is found allowing to deduce the spatial coherence outer scale L_0 and the Fried parameter r_0.

1. INTRODUCTION.

One of the basic problems in solar observations is the estimation of the optical transfer function (*OTF*) that describes the influence of the Earth's atmosphere on the observed images (Labeyrie, 1970). Due to the lack of point sources, solar limb observations (Druesne et al, 1983) or known structure on solar surface (Molodij and Rayrole, 1997) may serve as reference during the observations. Theoretical expressions of the *OTF* deduced from models of wave-front propagation through atmospheric turbulence in case of long-exposure frames have been established (Fried 1966; Roddier 1981). These expressions depend on the so-called Fried parameter r_0, which estimates the energy of the mean atmospheric turbulence. More recently, a new theoretical expression of long-exposure point spread function (*psf*) deduced from Von Karman model was established (Conan, 2000). This model depends on two optical atmospheric parameters: the Fried parameter r_0 and the spatial coherence outer scale L_0. The knowledge of this last parameter is of major interest in astronomy mainly for optimization of high angular resolution techniques (speckle interferometry, long baseline interferometry, adaptive optics). Several methods have been proposed to estimate the spatial coherence outer scale L_0 in the case of nighttime observations. Most of them are based on a statistical analysis of the Angle-of-Arrival (*AA*) fluctuations (Tallon, 1989; Borgnino 1989). A more detailed theoretical study associated to numerical simulations led to propose new techniques allowing L_0 estimation from its effects on the variance and the covariance of the *AA* fluctuations (Borgnino 1990, Borgnino *et al.* 1992, Ziad *et al.*, 1994). A Generalized Seeing Monitor (GSM) has then been built (Martin et al, 1994) allowing evaluation of many astronomical sites: La Silla, Maydanak, Cerro Pachon, Cerro Paranal (Ziad *et al*., 2000). For daytime observations, L_0 values are not very well known and its estimation is of great interest in order to evaluate optical effects induced by atmospheric turbulence on solar images. A seeing monitor is then useful and MISOLFA (Moniteur d'Images Solaires Franco-Algérien, still under construction) is built in this goal (http://www-astro.unice.fr). It is founded on the statistical analysis of *AA* fluctuations. MISOLFA is a generalized daytime seeing monitor that will observe together with experiments based at Calern Observatory (Observatoire de la Côte d'Azur - *OCA*) and dedicated to solar diameter measurements (solar astrolabe, DORaySOL (Définition et Observation du Rayon SOLaire) and soon SODISM II (SOlar Diameter Imager and Surface Mapper), replica of PICARD experiment, which will observe in space in 2006 (http://www-projet.cst.cnes.fr:8060/PICARD/Fr/). MISOLFA will give in real time estimations of the coherence parameters characterizing wave-fronts degraded by atmospheric turbulence (Fried's parameter r_0, size of the isoplanatic patch θ_0, spatial coherence outer scale L_0 and atmospheric correlation times) but also estimation of optical turbulence profiles.

In this paper, we propose a new method to estimate simultaneously the Fried parameter r_0 and the spatial coherence outer scale L_0 for daytime observations. It is based on the comparison between the one-dimensional long-exposure *psf* deduced from solar limb observations with the theoretical expression obtained in the case of the Von Karman model. The method is first developed using numerical simulation. It is then tested with experimental data performed at the Calern Observatory astrolabe (*OCA*) (Laclare et al, 1996).

2. EXPOSED METHOD, NUMERICAL SIMULATION

* Centre de Recherche en Astronomie Astrophysique et Géophysique, CRAAG – *Observatoire d'Alger*, BP 63 Bouzaréah 16340 Alger Algérie; phone 00 21321904460; fax 00 213904458; Email : irbah@unice.fr; ** Université de Nice – Sophia Antipolis, UMR n°6525 Astrophysique, Parc Valrose, 06108 Nice Cedex 2 France; fax 00 33492076321

2.1 Calculation of the one-dimensional long-exposure *psf* from simulated data

Several steps are needed to calculate the one-dimensional long-exposure *psf* according to Fried's terminology (Fried, 1966) from simulated solar data. In the following, we will denote the *psf* and the corresponding *OTF* by $R_{LE\text{-}Fried}(x)$ and $H_{LE\text{-}Fried}(f)$ where x and f are respectively space and frequency variables. The needed steps are the simulation of a synthetic image of the Sun limited to the telescope field of view, the randomly perturbed wave-front synthesis and solar image as obtained through the atmospheric turbulence in the case of a field wider than the isoplanatism angle. The model assumes that the optical effects induced by the whole terrestrial atmosphere may be due to an unique layer situated at a distance h above the telescope pupil; h is a parameter of the model.

2.1.1 Synthetic image of the Sun

A synthetic image of the Sun as obtained in space, is built using the single parameter model of mean solar limb darkening function proposed by Hestroffer and Magnan (1998) and given by:

$$I(\mu)= 1- (1-\mu)^{\alpha},\ \alpha \in R \quad \text{where} \quad \mu = \cos(\theta) = (1-r^2)^{1/2} \tag{2.1}$$

θ represents the angle between a Sun's radius vector and the line of sight.

$\theta=0$ corresponds to the center of the disk and $\theta= \pi/2$ to the solar edge. For observation with wavelength λ equal to 660 nm, the constant α is equal to 0.40.

Figure 1(a) shows the limb darkening function computed from equation 2.1 and Figure 1(b) the simulated image of the Sun as it can be obtained in space. The image size is equal to 64 by 64 pixels.

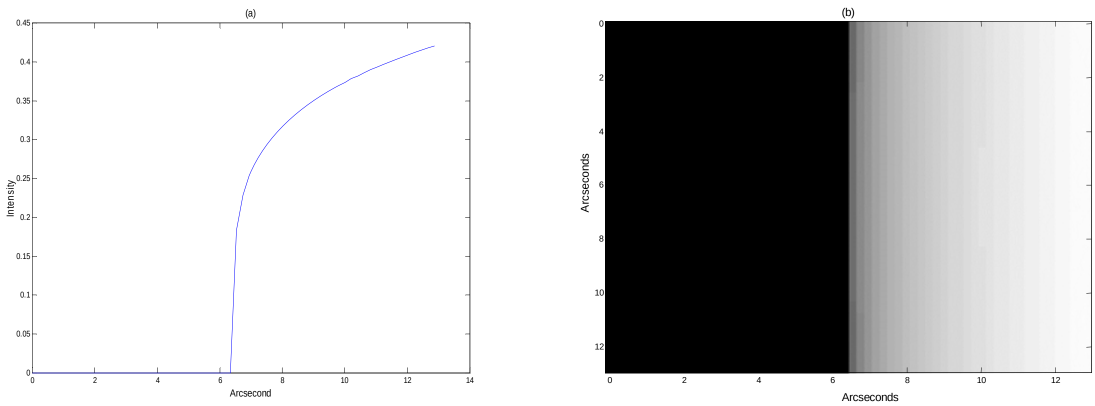

Figure 1: Solar limb darkening function (a) and the synthetic solar image (b)

2.1.2 Simulation of the phase screens using Nakajima method

In the near – field approximation and assuming the Von Karman model, the spectral density of the phase fluctuations at the aperture plane of the telescope is given by (Voitsekhovich, 1995, Ziad et al., 2000):

$$W_{\varphi}(f)=0.0229 r_0^{-5/3}\left(f^2+1/L_0^2\right)^{-11/6} \tag{2.2}$$

where $f=\sqrt{f_x^2+f_y^2}$ is the spatial frequency modulus, r_0 the Fried parameter and L_0 the wave-front outer scale.

We use equation (2.2) and the Nakajima method (Nakajima 1998; Borgnino et al., 1992) to generate random wave-fronts. Figure 2 represents a random phase screen simulated for r_0 = 5 cm and L_0 = 0.5 m.

2.1.3 Simulation of the solar image in absence of isoplanatism

We use the generated random phase screen to build solar images as recorded through the atmospheric turbulence in absence of isoplanatism. For the different points of the object field (synthetic image of the Sun), the telescope aperture projects itself onto different regions of the remote layer of turbulence (phase screen); for each of them a different *psf* is computed and added in the focal plane of the telescope with the intensity proportional to the object source (Beaumont et al., 1996).

Denoting $O(\alpha,\beta)$ the brightness intensity of the object and $S(x,y,\alpha,\beta)$ the instantaneous *psf* at the focus of the telescope, a point of the object produces in the focal plane of the telescope an intensity of the form:

$$O(\alpha,\beta)S(x,y,\alpha,\beta) \quad \text{with} \quad S(x,y,\alpha,\beta)=\left|FT[\exp(i\varphi(u,v))P(u-h\alpha,v-h\beta)]\right|^2 \tag{2.3}$$

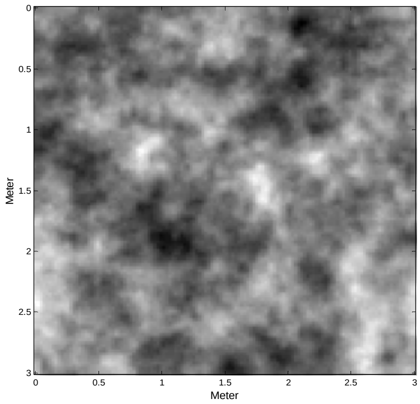

Figure 2: Phase screen sample generated for r_0 = 5 cm and L_0 = 0.5 m

where (α,β), (u,v), *and* (x,y) are coordinates respectively in object, pupil and image planes.
$\varphi(u,v)$ and $P(u,v)$ are respectively the random phase and amplitude of the pupil function; *FT* denotes the Fourier transform.
The image $I(x,y)$ at the focal plane is the addition in intensity of all these contributions (Figure 3):

$$I(x,y)=\int\int i(x,y,\alpha,\beta)d\alpha\, d\beta=\int\int O(\alpha,\beta)S(x,y,\alpha,\beta)d\alpha\, d\beta \qquad (2.4)$$

2.2 Calculation of $R_{LE\text{-}Fried}$ (x)

Using the previous developments, many sequences of solar images have been simulated in various observation conditions defined by the Fried parameter r_0 and the wave-front outer scale L_0.
From each simulated image (Figure 4 a), a solar edge constituted with the inflexion points of the solar limb function given by each CCD line is extracted. A parabolic fit is then made through the inflexion points and the coefficients a, b and c of the parabola estimated (Figure 4 a). If x_i and y_i are the co-ordinates of the solar edge points in the camera plane, we can write:

$$y_i=ax_i^2+bx_i+c \qquad (2.5)$$

The maximum (or minimum) of the parabola is given by:

$$x_s=\frac{-b}{2a}\ , \qquad y_s=\frac{-(b^2-4ac)}{4a} \qquad (2.6)$$

and the derivative solar image (Figure 4 b) corrected from the curvature effect is written as (Figure 4 c):

$$Icc(x,y)=I(x,y-y_i-y_s) \qquad (2.7)$$

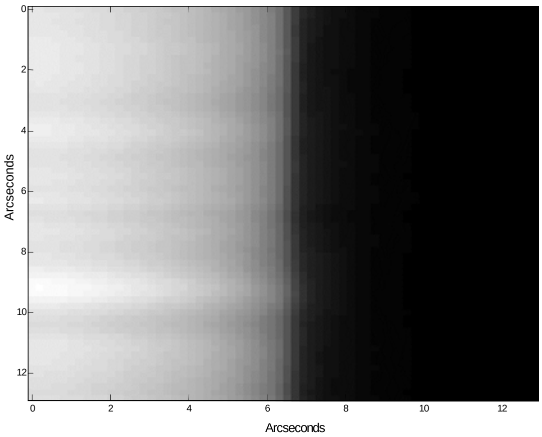

Figure 3: Simulated image of the Sun in absence of isoplanatism

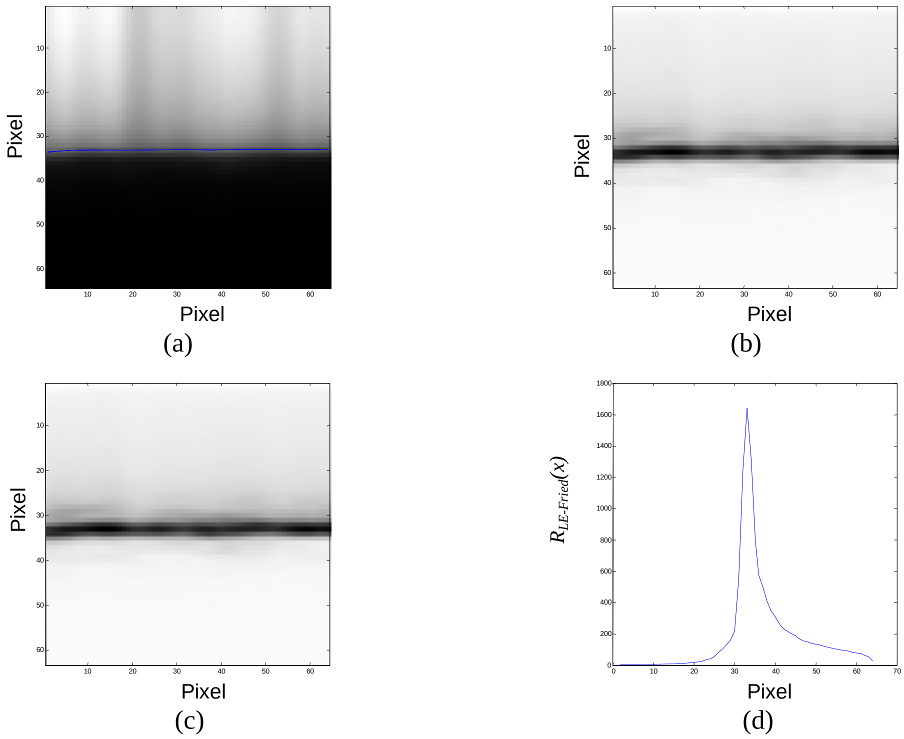

Figure 4: (a): Simulated image of the Sun with its edge fitted by a parabola (1pixel = 0.2 arcsecond). (b): The first derivative. (c): The first derivative corrected from the curvature effect. (d):The long-exposure *psf* ($R_{LE\text{-}Fried}$ (x)) distorted by the solar limb darkening

Under some statistical assumptions (stationarity, ergodicity…), the one-dimensional long-exposure *psf* according to Fried's definition $R_{LE\text{-}Fried}(x)$ is obtained by the summation of all the lines of $I_{CC}(x, y)$ (Figure 4 d).

$$R_{LE-Fried}(x)=\sum_y I_{CC}(x,y) \quad (2.8)$$

2.3 Theoretical long-exposure *psf*

The long - exposure *OTF* of the whole system instrument – atmosphere is given by (Roddier, 1981):

$$<\hat{F}(\vec{f})>=C_\psi(\vec{f}).\hat{F}_T(\vec{f}) \quad (2.9)$$

where C_ψ is the second order moment of the complex amplitude.

Using the Von Karman model, it is expressed as (Conan, 2000):

$$C_\psi(\vec{f})=\exp\left\{-\frac{\Gamma(11/6)}{2^{5/6}\pi^{8/3}}\left[\frac{24}{5}\Gamma(6/5)\right]^{5/6}\left(\frac{r_0}{L_0}\right)^{-5/3}\times\left[\frac{\Gamma(5/6)}{2^{1/6}}-\left(2\pi\frac{\lambda f}{L_0}\right)^{5/6}K_{5/6}\left(2\pi\frac{\lambda f}{L_0}\right)\right]\right\} \quad (2.10)$$

$K_{5/6}(r)$ is the modified Bessel function of second kind known as McDonald's function and $\Gamma(s)$ the gamma function.

$\hat{F}_T(\vec{f})$ is the telescope *OTF* :

$$\hat{F}_T(\vec{f})=\frac{2}{\pi}\left[ar\cos\left(\frac{\lambda f}{D}\right)-\frac{\lambda f}{D}\sqrt{1-\left(\frac{\lambda f}{D}\right)^2}\right] \quad (2.11)$$

The image is thus conditioned by the quality of the *psf* (Figure 5):

$$<F(\alpha)>=FT^{-1}[<\hat{F}(f_x,0)>] \quad (2.12)$$

where FT^{-1} denotes the inverse Fourier transform.

2.3 Comparison of the simulated *psf's* with the Von Karman model

The *psf's* obtained from the simulation method are compared to the theoretical ones obtained from equation 2.12 (Figure 6). We observe in the figure a good agreement between the simulation and theory. The simulated data points follow closely the profile expected from the Von Karman turbulence model.

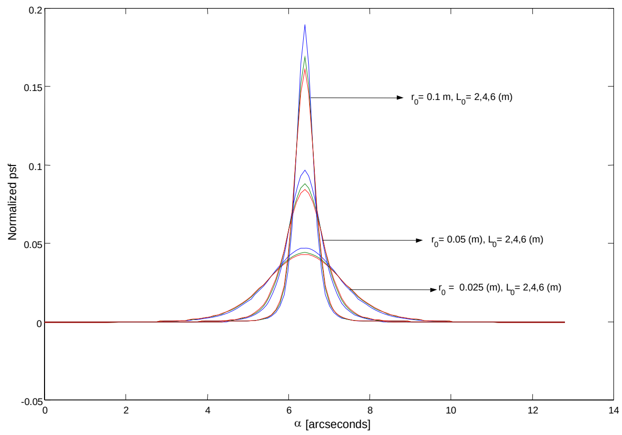

Figure 5: Long-exposure *psf's* obtained from the theoretical model for various values of r_0 and L_0. For each curve family L_0 parameter is increasing from the bottom to the top (pupil diameter D = 25 cm, focal length of the telescope F = 10 m, 1 pixel = 0.2 arcsecond).

For each *psf* simulated under given observation conditions (r_{0sim} and L_{0sim}), we determine using an iterative procedure, the Fried parameter and the outer scale values ($r_{0\,cal}$ and $L_{0\,cal}$) of the Von Karman's theoretical *psf* model corresponding to the best fit in the least square sense. In order to check the performance of the method, we calculate for each parameter the relative difference:

$$R_1 = \left| \frac{r_{0sim} - r_{0cal}}{r_{0sim}} \right| \quad \text{and} \quad R_2 = \left| \frac{L_{0sim} - L_{0cal}}{L_{0sim}} \right| \tag{2.13}$$

For a given value set (r_{0sim} , L_{0sim}), R_1 and R_2 are computed using 1000 samples. The numerical simulation results show a good efficiency of the method for parameter estimation, the relative difference do not exceed a few percents. However, this assumes the wave-front outer scale L_0 to be somewhat smaller than the phase screen length by a factor 3.
We will apply now the method to experimental data recorded at the Calern Observatory astrolabe (*OCA*).

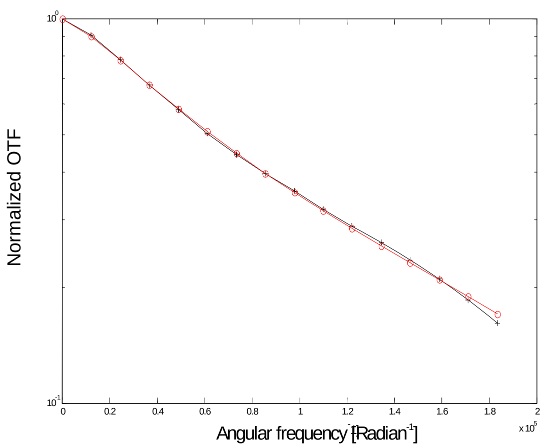

Figure 6: The simulated OTF (crosses) compared to Von Karman theoretical model (circles): a good agreement is observed.

3. APPLICATION TO EXPERIMENTAL DATA

3.1 Observations

These data have been performed with the solar astrolabe of Calern Observatory during May 1997. They consist in image sequences used for solar diameter measurements. Each sequence is made of 100 alternatively direct and reflected images, recorded at a rate of 4 images per second (Laclare et al, 1996). Each image is taken with a CCD camera having an integration time of 20 ms (Figure 7). Its size is some 101 by 256 rectangular pixels, which corresponds to a field on the sky of 75 by 287 arcsecond squares. The images are then *cleaned* by means of wavelet technique in order to remove all impurities (Irbah et al, 1999). The reflected image being generally worse than the direct ones due to the additional reflection on the mercury bath, we consider only the direct one in the analysis.

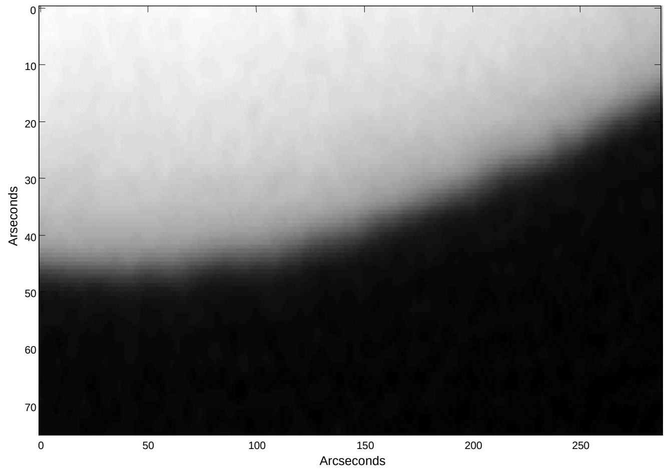

Figure 7: Image recorded with the solar astrolabe of Calern Observatory after being *cleaned*

3.2 Theoretical fit to the observed *OTF's*

Figure 8 shows an example of a comparison between the experimental *OTF* calculated from solar astrolabe data with Von Karman 's model. A good agreement is observed and the best fit, in the least -square sense, is obtained for r_0 = 1.8 cm and L_0 = 2.5 m.

At Calern Observatory, for observations made on May 22 1997, we have observed r_0 values in the range 0.5 to 2 cm and L_0 value 0.5 to 3 m. No obvious correlation is observed between these parameters (Figure 9).

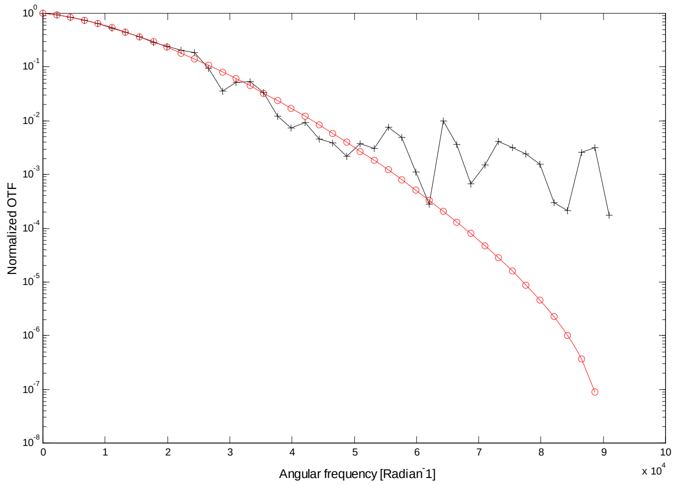

Figure 8: Comparison between the experimental *OTF's* calculated from solar astrolabe data (crosses) with Von Karman's model (circles): the best fit is obtained for r_0= 1.8 cm and L_0 = 2.5 m

4. CONCLUSION

A new method allowing simultaneous estimations of the Fried parameter r_0 and the spatial coherence outer scale L_0 for daytime observations was developed and tested on simulated solar data. This method is based on the comparison of the observed long-exposure *psf* according to Fried's definition with the theoretical one obtained using the Von Karman model.

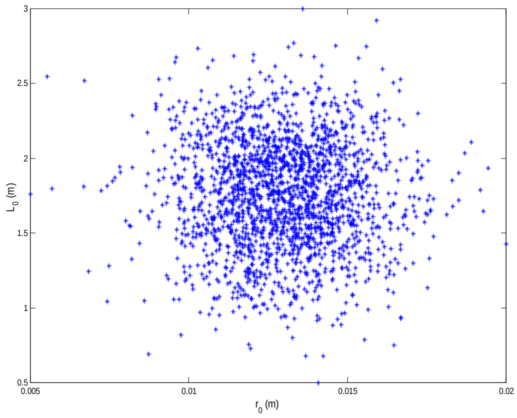

Figure 9: Outer scale L_0 versus Fried's parameter r_0

An iterative minimization method is used and provides the r_0 and L_0 parameters of the theoretical model corresponding to the best fit to the observations. The method was then applied to experimental data recorded at Calern Observatory astrolabe during May 1997. Results were consistent with the Von Karman statistics. Typical values of Fried's parameter r_0 and outer scale L_0 values were found ranging respectively from 0.5 to 2 cm and 0.5 to 3 m.

ACKNOWLEDGMENTS

This work has been performed with support of the French Foreign Affair Ministry in the framework of scientific co-operation between France and Algeria (contract 00 MDU 501).

REFERENCES

1. H. Beaumont, C. Aime, L. J. Sanchez, and H. Lanteri, 1996, ESO Workshop on Science with the VLTI, Garching, Germany
2. J. Borgnino, 1989, GISO 2 Forum, Nice Observatory
3. J. Borgnino, 1990, Applied Optics, 29, 13, 1883
4. J. Borgnino, F. Martin, and A. Ziad, 1992, Opt Comm, 91, 267
5. R. Conan, 2000, Thesis, Nice University, France.
6. P. Druesne, J. Borgnino, C. Aime, R. Petrov, and S. Kadiri, 1983, J. Optics, vol. 14, n^o 1, pp. 11-17.
7. D.L Fried, 1966, J. Opt. Soc. Am. 56, 1372.
8. D. Hestroffer, and C. Mafnan, 1998, A&A, 333, 338-342.
9. A. Irbah, M. Bouzaria, L. Lakhal, R. Moussaoui, J. Borgnino, F. Laclare, and C. Delmas, 1999, Solar Physics, vol. 185, Issue 2, p. 255-273.
10. A. Labeyrie, 1970, A&A 6, 85
11. F. Laclare, C. Delmas, J. P Coin, and A. Irbah, 1996, Solar Physics, 166, 211
12. F. Martin, A. Ziad, R. Conan, J. Borgnino, and A. Tokovinin, 2000, IAU Site Testing, November 13-17, 2000, Marrakech, Morocco.
13. G. Molodij, and J. Rayrole, 1997, A&A. Supp. Ser, 128, 229-244
14. T. Nakajima, 1988, J Opt Soc of Am, Issue 9, vol. 5, p., 1477-1491
15. F. Roddier, 1981, Progress in Optics, 19, 109
16. M. Tallon, 1989, Thesis, Nice University, France
17. V. Voitsekovich, 1995, J. Opt. Soc. Am. A 12, 1346-1353
18. A. Ziad A, J. Borgnino, F. Martin, and A. Agabi, 1994, A&A, 282, 1021.
19. A. Ziad, R. Conan, A. Tokovinin, F. Martin, and J. Borgnino, 2000, Applied Optics, 39, 5415-5425